Integrated Platform for Linezolid Combinations Against Rifampicin-Resistant Mycobacterium tuberculosis: Synergy, Macrophage Apoptosis, and Immune Modulation

Running Title: In Vitro Platform for LZD-Based Combination Testing in RR-TB

Dan Cui*, Na Li, Xinxin Ren

Department of Tuberculosis, Hebei Provincial Key Laboratory of Pulmonary Disesse, Hebei Chest Hospital, Shijiazhuang, Hebei, 050041,China.

*Corresponding Author: Dan Cui.

Department of Tuberculosis, Hebei Chest Hospital,372 Shengli North Street, Shijiazhuang,Hebei, 050041, China.

TEL:86-0311-86911077; Email: DanCui6982@163.com

Abstract

Objective: To establish an integrated in vitro evaluation platform for identifying effective antibiotic combinations against rifampicin-resistant Mycobacterium tuberculosis (RR-TB), by simultaneously assessing synergistic drug interactions, intracellular bactericidal activity, macrophage apoptosis, and cytokine responses. Using this platform, we investigated the combinatory potential of linezolid (LZD) with five second-line antitubercular agents.

Methods: The minimum inhibitory concentrations (MICs) of LZD and five second-line drugs were determined using the Alamar Blue microplate assay. Drug–drug interactions between LZD and cycloserine (CS), clofazimine (CFZ), bedaquiline (BDQ), moxifloxacin (MFX), or levofloxacin (LFX) were evaluated using checkerboard microdilution analysis. Drug pairs demonstrating in vitro synergy were further examined in a macrophage infection model. Intracellular bacterial burden was quantified by colony-forming unit (CFU) enumeration. Macrophage apoptosis was assessed using flow cytometry, and cytokine production (IL-12/23 p40, TNF-α, IL-6, and IL-10) was analyzed to characterize immune modulation.

Results: LZD demonstrated synergistic interactions with CS and CFZ, whereas no synergy was observed with BDQ, MFX, or LFX. The synergistic combinations LZD+CS and LZD+CFZ significantly reduced intracellular CFU counts, enhanced macrophage apoptosis, and altered cytokine responses, characterized by increased TNF-α and decreased IL-10 levels in infected macrophages.

Conclusion: This study presents a comprehensive and mechanistically informative in vitro methodology for evaluating antibiotic combinations against RR-TB. The platform effectively integrates drug synergy testing with assessments of intracellular killing, apoptosis induction, and immune modulation, offering a promising approach for preclinical screening of novel anti-TB therapeutic strategies.

Keywords: Rifampicin-resistant tuberculosis; Linezolid; Synergistic combinations; In vitro evaluation platform; Macrophage apoptosis; Cytokines

1.Introduction

Rifampicin-resistant tuberculosis (RR-TB) represents one of the most formidable challenges in global infectious disease control, with approximately 400,000 new cases annually and a mortality rate approaching 40% [1]. The emergence of drug-resistant Mycobacterium tuberculosis (MTB) strains has fundamentally altered the therapeutic landscape, necessitating novel treatment strategies that extend beyond traditional monotherapy approaches [2,3]. Despite the availability of second-line anti-tuberculosis agents, treatment success rates for RR-TB remain disappointingly low at approximately 55%, highlighting an urgent need for optimized combination therapies [4].

Linezolid (LZD), the first synthetic oxazolidinone antibiotic, has emerged as a cornerstone drug in RR-TB treatment regimens. Its unique mechanism of action—binding to the 50S ribosomal subunit and blocking the formation of the 70S initiation complex—confers minimal cross-resistance with other antimicrobials, making it particularly valuable against drug-resistant strains [5,6]. Recent clinical trials have demonstrated that LZD-containing regimens achieve sputum culture conversion rates exceeding 75% in patients with extensively drug-resistant tuberculosis, leading to its reclassification as a Group A drug by the World Health Organization [7,8].

However, the optimal combination partners for LZD remain incompletely defined. While current guidelines recommend combining LZD with bedaquiline, clofazimine, cycloserine, or fluoroquinolones, the mechanistic basis for these combinations and their differential efficacy has not been systematically evaluated [9,10]. Understanding the synergistic potential of specific drug combinations is crucial for maximizing therapeutic efficacy while minimizing the emergence of additional resistance.

Beyond direct antimicrobial effects, the host immune response plays a pivotal role in determining treatment outcomes in tuberculosis. MTB's intracellular lifestyle within macrophages presents a formidable barrier to antimicrobial therapy, as the pathogen actively manipulates host cell death pathways to ensure its survival [11]. Recent evidence suggests that effective anti-TB drugs may function not only through direct bacterial killing but also by modulating host immune responses, particularly the balance between pro-inflammatory and anti-inflammatory cytokines [12]. The TNF-α/IL-10 ratio has emerged as a critical determinant of macrophage fate during MTB infection, with

TNF- α promoting protective apoptosis while IL-10 suppresses this response and facilitates bacterial persistence [13,14].

The interplay between antimicrobial activity and immunomodulation represents an underexplored dimension of combination therapy. While previous studies have examined the bactericidal effects of LZD combinations [15], the impact of these regimens on host immune responses, particularly macrophage apoptosis and cytokine production, remains poorly characterized. This knowledge gap limits our ability to rationally design combination therapies that harness both antimicrobial and immunological mechanisms.

Therefore, this study aimed to systematically evaluate the synergistic antimicrobial effects of linezolid combined with five key second-line anti-TB agents against rifampicin-resistant MTB strains. Furthermore, we investigated the immunological mechanisms underlying these combinations, with particular focus on their ability to modulate macrophage apoptosis and reshape cytokine profiles. Our findings provide mechanistic insights that could guide the optimization of combination therapies for drug-resistant tuberculosis.

2.Materials and Methods

2.1. Microplate Alamar Blue Assay (MABA)

The standard strain of Mycobacterium tuberculosis H37Rv (ATCC 27295) was obtained from the Key Laboratory of Pulmonary Diseases, Hebei Chest Hospital, while three clinical rifampicin-resistant MTB isolates (RR-TB-1, RR-TB-2, RR-TB-3) were provided by the institution’s Key Laboratory. The human monocytic cell line THP-1 (ATCC: TIB-202), derived from peripheral blood, was sourced from the Beijing Tuberculosis and Thoracic Tumor Research Institute. Frozen MTB strains were subcultured on modified neutral Löwenstein–Jensen medium and incubated at 37°C for 3–4 weeks.

Fresh colonies were scraped, homogenized by vortexing in a bacterial grinding tube for 20 seconds, adjusted to McFarland standard 1.0, and subsequently diluted 1:20 in Middlebrook 7H9 broth supplemented with 10% OADC. A 96-well plate was prepared by serially diluting anti-tuberculosis agents in 10% OADC-enriched 7H9 medium to achieve

final concentrations of 0.015, 0.03, 0.06, 0.125, 0.25, 0.5, 1.0, 2.0, 4.0, 8.0, and 16.0 μg/mL, with 100 μL of each concentration added per well. The diluted bacterial suspension was then added to the drug-containing wells, alongside a positive control group (bacteria without drugs) and a negative control group (medium without bacteria). Plates were incubated at 37°C for 9 days. Subsequently, 20 μL of Alamar Blue solution and 50 μL of 5% Tween-80 were added to each well.

After an additional 24-hour incubation at 37°C, results were interpreted based on color change: a shift from blue to pink indicated bacterial growth. The minimum inhibitory concentration (MIC) was defined as the lowest drug concentration that prevented color change. The MIC50, representing the concentration at which 50% of the bacterial population was inhibited, reflects the drug's antibacterial potency—lower MIC50 values indicate stronger inhibitory activity.

2.2. Checkerboard Assay for Drug Synergy Testing

The checkerboard microdilution method was employed to assess the in vitro combinatorial effects of LZD with five antibiotics: cycloserine (CS), bedaquiline (BDQ), clofazimine (CFZ), moxifloxacin (MFX), and levofloxacin (LFX). LZD was tested at 1/4×, 1/2×, 1×, and 2× its MIC in combination with each of the five drugs at the same respective concentrations. The procedures were identical to those described above. Bacterial growth was monitored under various combinatory conditions. Monotherapy groups for LZD and each of the five antibiotics, along with both positive and negative controls, were included. The 96-well plates were incubated at 37°C for 18–24 hours, after which bacterial growth was evaluated. All experiments were conducted in triplicate. The MIC of the combination was defined as the lowest concentration in wells showing no visible bacterial growth. The fractional inhibitory concentration index (FICI) was calculated using the formula: FICI = (MIC_A_combination / MIC_A_alone) + (MIC_B_combination / MIC_B_alone). Interpretation of FICI values was based on established criteria: FICI $\leq$ 0.5 indicated synergism, 0.5 < FICI $\leq$ 1 indicated an additive effect, 1 < FICI $\leq$ 4 indicated indifference, and FICI > 4 indicated antagonism (Odds, 2003).

2.3. Intracellular CFU Assay

THP-1-derived macrophages were infected with H37Rv or RR-TB (MOI 1:10), followed by treatment with LZD alone or in combination with CS/CFZ at MIC, 10×MIC, or 20×MIC for 4–48 hours. Cells were lysed with 0.5% Triton X-100, serially diluted, plated on 7H10 agar, and incubated for 3–4 weeks for CFU counting. Experiments were performed in triplicate.

2.4. Flow Cytometry for Apoptosis

Flow cytometry was employed to assess apoptosis rates using the Annexin V-Alexa Fluor 647/PI dual-staining apoptosis detection kit, following the manufacturer's protocol. Cells were harvested at five different time points: 1, 3, 6, 12, and 24 hours post-treatment. After two washes with PBS, cells were digested with trypsin as per the instructions and neutralized with complete medium. The binding buffer provided in the kit was diluted 1:4 with deionized water for subsequent use. Cells were then washed twice with pre-chilled PBS, resuspended in 300 µL of binding buffer, and adjusted to a final concentration of 1×10^6 cells/mL.

For staining, 100 µL of the cell suspension was transferred into sterile 1.5 mL centrifuge tubes, followed by the addition of 5 µL Annexin V-Alexa Fluor 647. Samples were incubated for 5 minutes at room temperature in the dark, after which 10 µL of 20 µg/mL propidium iodide (PI) solution was added to each tube. Subsequently, 700 µL of PBS was added and mixed by gentle inversion. Apoptosis rates were analyzed using a C6 flow cytometer. Quality control measures included triplicate experiments for each bacterial strain, with the most consistent result from the three used for analysis. The H37Rv strain was used as an internal quality control in every assay.

2.5. Multiplex Cytokine Detection (Luminex Assay)

Cytokine levels of IL-12/23 p40, TNF-α, IL-6, and IL-10 in cell culture supernatants were quantified using a Magnetic Luminex® Assay following the manufacturer's protocol. Briefly, 200 µL of assay buffer was added to each well for plate pre-wetting, followed by sealing and shaking at room temperature for 10 minutes; buffer was discarded and residual liquid removed by inversion onto absorbent paper. For sample loading, 50 µL of respective reagents were added to background, standard, and control wells, while 25 µL of assay buffer and 25 µL of sample were added to sample wells.

Premixed magnetic beads (25 µL/well) were added with continuous vortexing of the bead suspension. Plates were sealed, covered with a metal plate to protect from light, and incubated overnight (16–18 h) at 4 °C with agitation. Following incubation, plates were shaken for an additional 30–60 minutes at room temperature, washed three times with 200 µL wash buffer using a magnetic plate for bead retention. Subsequently, 50 µL of detection antibody (pre-equilibrated to room temperature) was added to each well, followed by 1-hour incubation at room temperature with agitation in the dark.

Without removing the detection antibody, 50 µL of Streptavidin-PE was added to each well, and plates were incubated for 30 minutes under the same conditions. After washing as described, 150 µL of sheath or drive fluid was added to each well, and plates were shaken for 5 minutes to resuspend beads. Data acquisition was performed on a Luminex® 200™ system, and cytokine concentrations were calculated using xPONENT® 3.0 software based on standard curves. All assays were performed in triplicate.

2.6. Statistical Analysis

Data were analyzed using SPSS v21.0. Continuous variables were expressed as mean ± SD or median (P25–P75) and compared using t-tests or Mann–Whitney U tests, as appropriate. Categorical variables were compared using χ^2 tests. Logistic regression was used to identify risk factors for LZD-associated adverse effects. A two-sided P-value <0.05 was considered statistically significant.

3.Results

3.1. Synergistic Effects of LZD with CS and CFZ

The MICs for H37Rv and RR-TB strains were: LZD 1.0 µg/mL, CS 2.0 µg/mL, MFX 0.03 µg/mL, BDQ 0.06 µg/mL, CFZ 0.25 µg/mL, and LFX 0.25 µg/mL.

At 1/4 MIC LZD, combined with full MIC doses of BDQ, MFX, or LFX, ≥90% inhibition was achieved. Combinations with 1/2 MIC CS or CFZ also achieved ≥90% inhibition.

The FICI values were: LZD+MFX = 1.25, LZD+CS = 0.75, LZD+CFZ = 0.75, LZD+LFX = 1.25, LZD+BDQ = 1.25, indicating synergy only with CS and CFZ. These

findings were consistent in both standard and resistant strains.

3.2. LZD + CFZ or CS Reduces Intracellular CFU, with Stronger Effect for CFZ

As shown in Figure 1 and Table 1, LZD+CS at MIC levels significantly reduced intracellular CFU counts in both H37Rv and RR-TB macrophage models over 4–48 hours ($P < 0.05$), with the lowest counts at 48 h.

Higher doses (10× and 20× MIC) led to further reductions ($P < 0.05$). The CFU-reducing trends for LZD+CFZ were similar. However, LZD+CFZ showed slightly stronger intracellular killing than LZD+CS in both models.

3.3. Early Increase and Late Decrease in Apoptosis After LZD + CS or CFZ Treatment

As shown in Figure 2 and Table 2, both LZD+CS and LZD+CFZ significantly increased macrophage apoptosis rates compared to control ($P < 0.05$). The LZD+CS group exhibited significantly higher apoptosis than LZD+CFZ at 1, 3, 6, and 12 h ($P < 0.05$); no difference was observed at 24 h.

Apoptosis peaked at early timepoints and decreased thereafter in both groups.

3.4. LZD + CS or CFZ Modulates Cytokine Profiles

IL-12/23 P40 levels increased significantly after LZD+CS or LZD+CFZ treatment compared to controls in both H37Rv and RR-TB groups (Figure 3, Table 3; $P < 0.05$).

TNF-α expression rose significantly at 4, 24, and 48 h in both treatment groups (Table 4; $P < 0.05$). In RR-TB strains, increases were significant only at 24 h.

IL-6 levels were lower in treated groups compared to controls post-treatment ($P < 0.05$) (Table 5).

For IL-10 (Table 6), LZD+CS significantly reduced levels at 4 and 24 h in both H37Rv and RR-TB models ($P < 0.05$), while LZD+CFZ had no statistically significant effect.

Discussion

Our study provides compelling evidence that linezolid exhibits selective synergistic interactions with cycloserine and clofazimine against rifampicin-resistant MTB, while demonstrating indifferent effects with bedaquiline and fluoroquinolones. The FICI values

of 0.75 for both LZD+CS and LZD+CFZ combinations indicate true synergy rather than mere additive effects, a finding with important implications for optimizing treatment regimens in RR-TB [16].

The selective nature of these synergistic interactions warrants careful consideration. The lack of synergy between LZD and fluoroquinolones (FICI = 1.25) is particularly noteworthy given that both drugs are frequently co-administered in clinical practice [17]. This finding aligns with recent epidemiological data showing high rates of fluoroquinolone resistance in MDR-TB strains—ranging from 30.4% to 51.8% across different regions—which may limit the utility of LZD-fluoroquinolone combinations [18–20]. In contrast, the robust synergy observed with CS and CFZ suggests these combinations merit prioritization in treatment regimens, particularly in settings with high fluoroquinolone resistance prevalence.

The intracellular killing assays revealed a critical dimension of these synergistic effects. Both LZD+CS and LZD+CFZ achieved progressive CFU reductions over 48 hours, with LZD+CFZ demonstrating slightly superior bactericidal activity. The dose-dependent enhancement observed at 10× and 20× MIC concentrations provides experimental support for the high-dose LZD strategies employed in some clinical protocols [21,22]. However, the substantial efficacy achieved at MIC levels suggests that lower, potentially less toxic doses may be sufficient when optimal combination partners are selected.

Our flow cytometry data uncovered distinct temporal patterns of macrophage apoptosis induced by the synergistic combinations. The LZD+CS combination triggered rapid and pronounced apoptosis within the first 12 hours, while LZD+CFZ induced a more gradual apoptotic response. This early apoptotic burst with LZD+CS may reflect activation of specific pro-apoptotic signaling cascades, potentially involving oxidative stress pathways similar to those described for other antimicrobials [23]. The convergence of apoptosis rates at 24 hours suggests both combinations ultimately achieve similar endpoints through different kinetic pathways.

The cytokine profiling revealed sophisticated immunomodulatory effects that extend beyond direct antimicrobial activity. The significant elevation of IL-12/23 p40 by both

combinations indicates enhancement of Th1-mediated immunity, which is essential for mycobacterial control [24]. The concurrent increase in TNF-α expression is particularly significant given its dual role in granuloma maintenance and induction of protective apoptosis in infected macrophages [25,26]. Previous studies have demonstrated that the TNF-α/IL-10 ratio critically determines the fate of MTB-infected macrophages, with higher ratios favoring bacterial clearance[27].

The differential effects on IL-10 production represent perhaps the most intriguing finding. While LZD+CS significantly suppressed IL-10 at multiple time points, LZD+CFZ showed no significant effect on this immunosuppressive cytokine. IL-10 is known to inhibit phagosome maturation and reduce pro-inflammatory responses, creating a permissive environment for MTB survival [28]. The ability of LZD+CS to simultaneously elevate TNF-α while suppressing IL-10 creates an immunological milieu strongly favoring bacterial clearance. This may explain why LZD+CS induced more rapid apoptosis despite LZD+CFZ showing slightly superior direct bactericidal activity.

The reduction in IL-6 levels observed with both combinations suggests mitigation of excessive inflammatory responses that can contribute to tissue damage [29]. This anti-inflammatory effect, combined with the pro-apoptotic and bactericidal activities, indicates that these combinations achieve a balanced therapeutic response—eliminating bacteria while limiting immunopathology.

Our findings align with recent clinical observations of improved outcomes with LZD-containing regimens [30,31]. The mechanistic insights provided here suggest that the clinical benefits of these combinations extend beyond simple additive antimicrobial effects. The synergistic bacterial killing combined with favorable immunomodulation creates a multi-pronged therapeutic approach that addresses both the pathogen and the subverted host response.

The implications for drug resistance are significant. Population-based studies indicate that MDR-TB strains resistant to second-line drugs are increasingly prevalent, with transmission rather than de novo resistance driving much of this burden [32–35]. The rapid bactericidal activity and immune enhancement observed with LZD+CS and LZD+CFZ combinations could potentially reduce the infectious period and limit

transmission opportunities. Moreover, the synergistic interactions may reduce the likelihood of resistance emergence by ensuring more complete bacterial killing [36].

These findings also provide insights into the mechanisms of MTB persistence. The pathogen's ability to manipulate host cell death pathways and cytokine responses represents a sophisticated survival strategy[37–39]. Our data suggest that effective combination therapies must counter these evasion mechanisms through both direct antimicrobial effects and restoration of protective immune responses. The differential immunomodulatory profiles of LZD+CS versus LZD+CFZ indicate that treatment selection could potentially be tailored based on individual patient immune status [40].

Several limitations should be acknowledged. Our in vitro system cannot fully recapitulate the complex granuloma microenvironment where oxygen tension, pH, and cellular composition influence drug activity and immune responses. The study examined acute treatment effects up to 48 hours, whereas clinical treatment extends over months. Long-term effects on bacterial persistence and resistance emergence require further investigation. Additionally, the THP-1 model, while valuable, may not fully reflect primary human macrophage responses.

Conclusion

LZD treatment for TB is associated with a range of adverse events. Female sex, older age, high dosage, prolonged treatment, and comorbidities are significant risk factors. LZD demonstrates synergistic effects with CS and CFZ but not with BDQ, MFX, or LFX. LZD+CS and LZD+CFZ combinations effectively inhibit MTB growth, potentially by promoting apoptosis of infected macrophages.

Ethics declarations

This study did not involve human participants or animals. The standard strain of Mycobacterium tuberculosis H37Rv (ATCC 27295) was obtained from the Key Laboratory of Pulmonary Diseases, Hebei Chest Hospital, and therefore did not require ethical approval.

Funding

This project was funded by Medical Science Research Project of Hebei [No.20260817].

Authors' contributions

D.C.: Conceptualization, Data curation, Formal analysis, Investigation, Methodology, Project administration,Writing - original draft, Writing - review & editing;

N.L.:Investigation, Formal analysis, Writing - review & editing;

X.X. R.: Conceptualization, Methodology, Investigation, Writing - review & editing.

Conflict of interest

All authors declare no conflict of interest.

Data availability

The data that support the findings of this study are not publicly available due to privacy reasons but are available from the corresponding author upon request.

Reference

1. World Health Organization. Drug-resistant TB. In: 1.3 Drug-resistant TB - Global Tuberculosis Report 2024. *Geneva: WHO* (2024). at <https://www.who.int/teams/global-programme-on-tuberculosis-and-lung-health/tb-reports/global-tuberculosis-report-2024/tb-disease-burden/1-3-drug-resistant-tb>
2. Kanabalan, R. D. *et al.* Human tuberculosis and Mycobacterium tuberculosis complex: A review on genetic diversity, pathogenesis and omics approaches in host biomarkers discovery. *Microbiol Res* **246,** 126674 (2021).
3. Dechow, S. J. & Abramovitch, R. B. Targeting Mycobacterium tuberculosis pH-driven adaptation. *Microbiology (Reading)* **170,** 001458 (2024).
4. Mohammadnabi, N. *et al.* Mycobacterium tuberculosis: The Mechanism of Pathogenicity, Immune Responses, and Diagnostic Challenges. *J Clin Lab Anal* **38,** e25122 (2024).
5. Conradie, F. *et al.* Bedaquiline-Pretomanid-Linezolid Regimens for Drug-Resistant Tuberculosis. *N Engl J Med* **387,** 810–823 (2022).
6. Elbarbry, F. & Moshirian, N. Linezolid-associated serotonin toxicity: a systematic review. *Eur J Clin Pharmacol* **79,** 875–883 (2023).
7. Howell, P. *et al.* Treatment of Rifampicin-Resistant Tuberculosis Disease and Infection in Children: Key Updates, Challenges and Opportunities. *Pathogens* **11,** 381 (2022).
8. Nyang'wa, B.-T. *et al.* Short oral regimens for pulmonary rifampicin-resistant tuberculosis (TB-PRACTECAL): an open-label, randomised, controlled, phase 2B-3, multi-arm, multicentre, non-inferiority trial. *Lancet Respir Med* **12,** 117–128 (2024).

9. Ding, P., Li, X., Jia, Z. & Lu, Z. Multidrug-resistant tuberculosis (MDR-TB) disease burden in China: a systematic review and spatio-temporal analysis. *BMC Infect Dis* **17,** 57 (2017).

10. Khan, M. A. *et al.* MDR-TB in Pakistan: Challenges, efforts, and recommendations. *Ann Med Surg (Lond)* **79,** 104009 (2022).

11. Howard, N. C. & Khader, S. A. Immunometabolism during Mycobacterium tuberculosis Infection. *Trends Microbiol* **28,** 832–850 (2020).

12. Salzer, H. J. F. *et al.* Personalized Medicine for Chronic Respiratory Infectious Diseases: Tuberculosis, Nontuberculous Mycobacterial Pulmonary Diseases, and Chronic Pulmonary Aspergillosis. *Respiration* **92,** 199–214 (2016).

13. Lemus, D. *et al.* Antituberculosis Drug Resistance in Pulmonary Isolates of Mycobacterium tuberculosis, Cuba 2012-2014. *MEDICC Rev* **19,** 10–15 (2017).

14. Simões, M. F., Ottoni, C. A. & Antunes, A. Mycogenic Metal Nanoparticles for the Treatment of Mycobacterioses. *Antibiotics (Basel)* **9,** 569 (2020).

15. Liu, C.-X., Zhao, X., Wang, L. & Yang, Z.-C. Quinoline derivatives as potential anti-tubercular agents: Synthesis, molecular docking and mechanism of action. *Microb Pathog* **165,** 105507 (2022).

16. Micheletti, V. C. D., Kritski, A. L. & Braga, J. U. Clinical Features and Treatment Outcomes of Patients with Drug-Resistant and Drug-Sensitive Tuberculosis: A Historical Cohort Study in Porto Alegre, Brazil. *PLoS One* **11,** e0160109 (2016).

17. Getahun, M., Blumberg, H. M., Ameni, G., Beyene, D. & Kempker, R. R. Minimum inhibitory concentrations of rifampin and isoniazid among multidrug and isoniazid

resistant Mycobacterium tuberculosis in Ethiopia. *PLoS One* **17,** e0274426 (2022).

18. Sharma, A. *et al.* Estimating the future burden of multidrug-resistant and extensively drug-resistant tuberculosis in India, the Philippines, Russia, and South Africa: a mathematical modelling study. *Lancet Infect Dis* **17,** 707–715 (2017).
19. Singh, P. K. & Jain, A. Limited Scope of Shorter Drug Regimen for MDR TB Caused by High Resistance to Fluoroquinolone. *Emerg Infect Dis* **25,** 1760–1762 (2019).
20. Gao, J. *et al.* Stepwise selection of mutation conferring fluroquinolone resistance: multisite MDR-TB cohort study. *Eur J Clin Microbiol Infect Dis* **40,** 1767–1771 (2021).
21. Wasserman, S., Meintjes, G. & Maartens, G. Linezolid in the treatment of drug-resistant tuberculosis: the challenge of its narrow therapeutic index. *Expert Rev Anti Infect Ther* **14,** 901–915 (2016).
22. Lee, J.-K. *et al.* Substitution of ethambutol with linezolid during the intensive phase of treatment of pulmonary tuberculosis: a prospective, multicentre, randomised, open-label, phase 2 trial. *Lancet Infect Dis* **19,** 46–55 (2019).
23. Bagheri-Yarmand, R. *et al.* Combinations of Tyrosine Kinase Inhibitor and ERAD Inhibitor Promote Oxidative Stress–Induced Apoptosis through ATF4 and KLF9 in Medullary Thyroid Cancer. *Molecular Cancer Research* **17,** 751–760 (2019).
24. Cox, D. J. *et al.* Inhibiting Histone Deacetylases in Human Macrophages Promotes Glycolysis, IL-1β, and T Helper Cell Responses to Mycobacterium tuberculosis. *Front Immunol* **11,** 1609 (2020).
25. Singh, P. *et al.* Computational modeling and bioinformatic analyses of functional

mutations in drug target genes in Mycobacterium tuberculosis. *Comput Struct Biotechnol J* **19,** 2423–2446 (2021).

26. Bakhtiyariniya, P., Khosravi, A. D., Hashemzadeh, M. & Savari, M. Detection and characterization of mutations in genes related to isoniazid resistance in Mycobacterium tuberculosis clinical isolates from Iran. *Mol Biol Rep* **49,** 6135–6143 (2022).
27. Tan, Z. M. *et al.* Novel Approaches for the Treatment of Pulmonary Tuberculosis. *Pharmaceutics* **12,** 1196 (2020).
28. Ramachandran, G. & Swaminathan, S. Safety and tolerability profile of second-line anti-tuberculosis medications. *Drug Saf* **38,** 253–269 (2015).
29. Jagielski, T. *et al.* A close-up on the epidemiology and transmission of multidrug-resistant tuberculosis in Poland. *Eur J Clin Microbiol Infect Dis* **34,** 41–53 (2015).
30. Lee, S.-M. *et al.* Resistance mechanisms of linezolid-nonsusceptible enterococci in Korea: low rate of 23S rRNA mutations in Enterococcus faecium. *J Med Microbiol* **66,** 1730–1735 (2017).
31. Tang, M. *et al.* The Properties of Linezolid, Rifampicin, and Vancomycin, as Well as the Mechanism of Action of Pentamidine, Determine Their Synergy against Gram-Negative Bacteria. *Int J Mol Sci* **24,** 13812 (2023).
32. Dodd, C. E., Pyle, C. J., Glowinski, R., Rajaram, M. V. S. & Schlesinger, L. S. CD36-Mediated Uptake of Surfactant Lipids by Human Macrophages Promotes Intracellular Growth of Mycobacterium tuberculosis. *J Immunol* **197,** 4727–4735

(2016).

33. Beutler, M. *et al.* Rapid Tuberculosis Diagnostics Including Molecular First- and Second-Line Resistance Testing Based on a Novel Microfluidic DNA Extraction Cartridge. *J Mol Diagn* **23,** 643–650 (2021).
34. Liebenberg, D., Gordhan, B. G. & Kana, B. D. Drug resistant tuberculosis: Implications for transmission, diagnosis, and disease management. *Front Cell Infect Microbiol* **12,** 943545 (2022).
35. Zhang, T. *et al.* The global, regional, and national burden of tuberculosis in 204 countries and territories, 1990–2019. *Journal of Infection and Public Health* **16,** 368–375 (2023).
36. Chen, Y. *et al.* Resistance to Second-Line Antituberculosis Drugs and Delay in Drug Susceptibility Testing among Multidrug-Resistant Tuberculosis Patients in Shanghai. *Biomed Res Int* **2016,** 2628913 (2016).
37. Coutinho, A. E. & Chapman, K. E. The anti-inflammatory and immunosuppressive effects of glucocorticoids, recent developments and mechanistic insights. *Mol Cell Endocrinol* **335,** 2–13 (2011).
38. Van't Hoog, A. H. *et al.* The potential of a multiplex high-throughput molecular assay for early detection of first and second line tuberculosis drug resistance mutations to improve infection control and reduce costs: a decision analytical modeling study. *BMC Infect Dis* **15,** 473 (2015).
39. Liang, Y.-N. *et al.* MiR-124 contributes to glucocorticoid resistance in acute lymphoblastic leukemia by promoting proliferation, inhibiting apoptosis and

targeting the glucocorticoid receptor. *The Journal of Steroid Biochemistry and Molecular Biology* **172,** 62–68 (2017).

40. Matlow, A. G., Harrison, A., Monteath, A., Roach, P. & Balfe, J. W. Nosocomial transmission of tuberculosis (TB) associated with care of an infant with peritoneal TB. *Infect Control Hosp Epidemiol* **21,** 222–223 (2000).

Figure legends

Figure 1. Intracellular CFU counts following treatment with LZD combined with CS or CFZ in RR-TB infection models. (A) CS + LZD, H37Rv reference strain; (B) CS + LZD, RR-TB strain; (C) CFZ + LZD, H37Rv reference strain; (D) CFZ + LZD, RR-TB strain. ***P < 0.001.

Figure 2. Apoptosis analysis of RR-TB-infected cells following treatment with LZD combined with CS or CFZ. (A) Flow cytometry analysis of cell apoptosis. The lower left quadrant indicates viable cells, the upper left quadrant represents necrotic or damaged cells, the upper right quadrant shows late apoptotic cells, and the lower right quadrant denotes early apoptotic cells. The total apoptosis rate is calculated as the sum of early and late apoptotic cells; (B) Quantification of apoptosis rates in RR-TB-infected cells treated with LZD+CS or LZD+CFZ. *P < 0.05, **P < 0.01, ***P < 0.001.

Figure 3. Cytokine expression levels (pg/mL) in RR-MTB infection models following treatment with LZD combined with CS or CFZ. (A) IL-12/23 p40, H37Rv reference strain; (B) IL-12/23 p40, RR-TB strain; (C) TNF-α, H37Rv reference strain; (D) TNF-α, RR-TB strain; (E) IL-6, H37Rv reference strain; (F) IL-6, RR-TB strain; (G) IL-10, H37Rv reference strain; (H) IL-10, RR-TB strain. P < 0.05, **P < 0.01, ***P < 0.001.

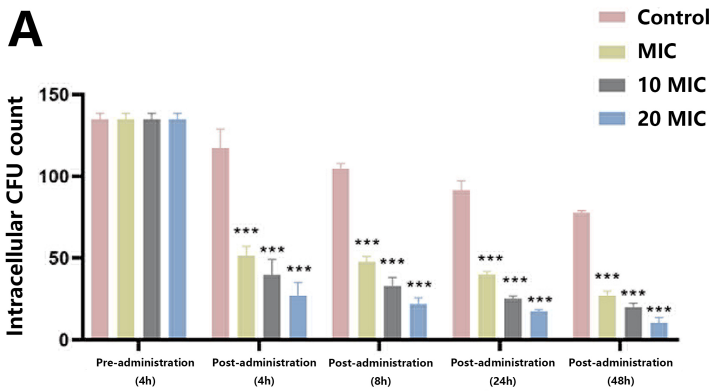

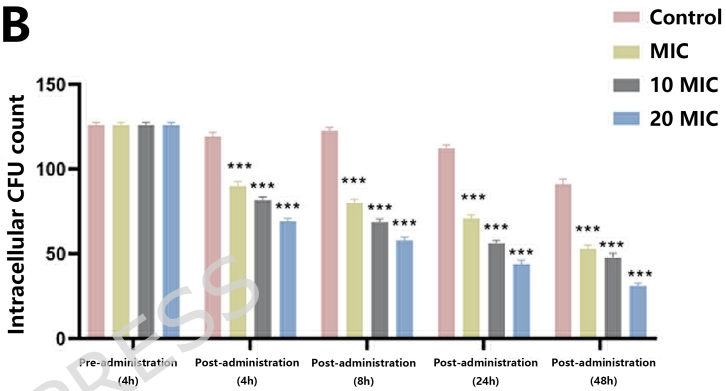

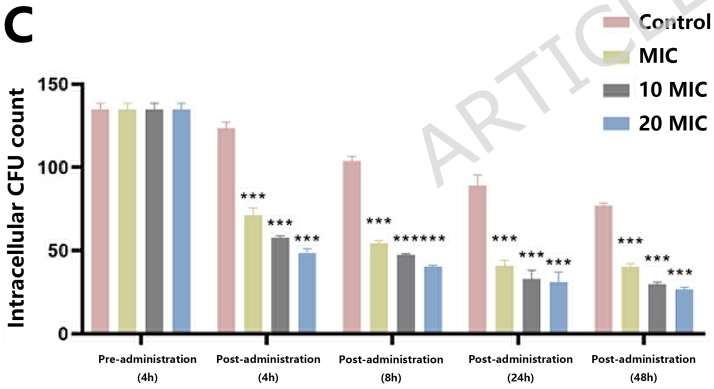

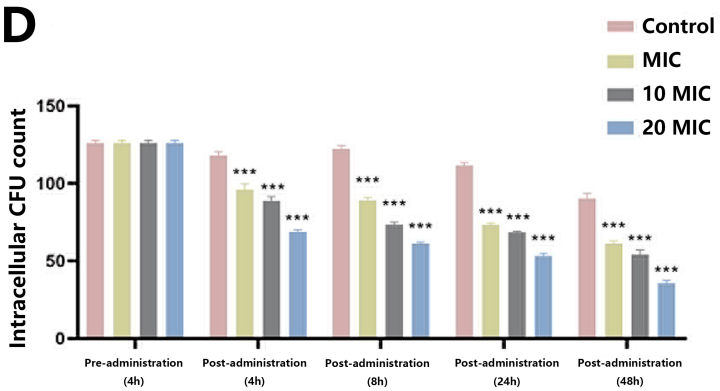

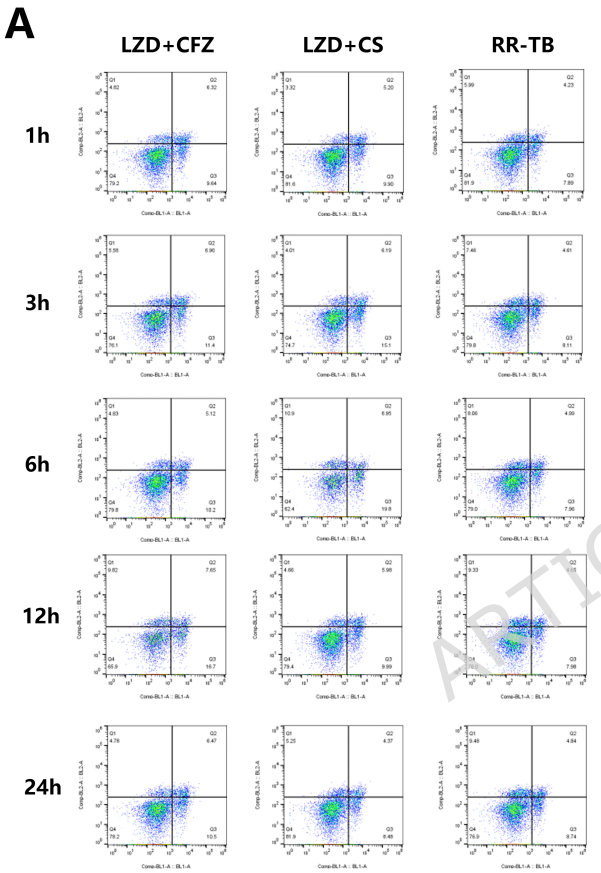

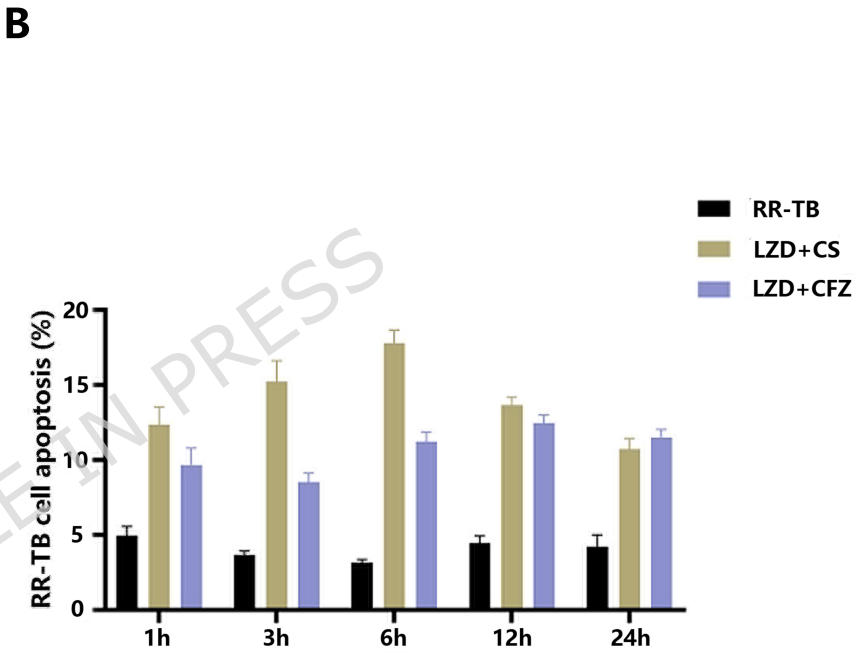

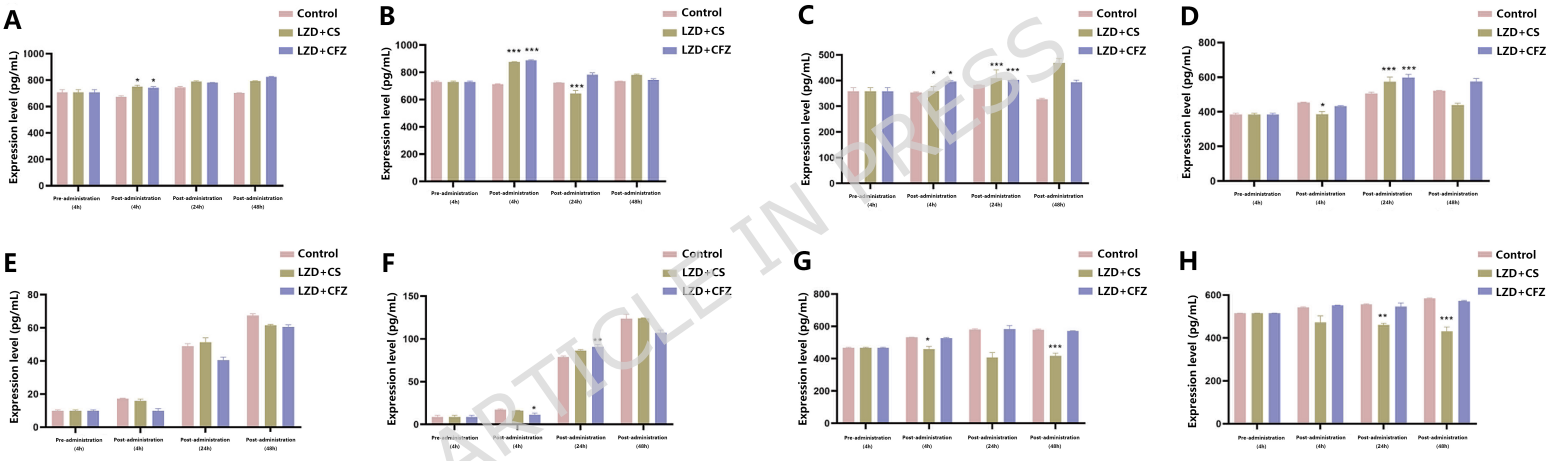

Table 1. Baseline Characteristics of Patients (N = 184)

	Group	Value, n (%) or Median (IQR)
Age (years)		34 (23.0-52.0)
Sex	Male	122 (66.3%)
	Female	62 (33.7%)
Comorbidities	No	88 (47.8%)
	Yes	96 (52.2%)
Duration of LZD use (days)		115.5 (52.0-246.8)
LZD dosage (mg)	≤ 600	136 (73.9%)
	> 600	48 (26.1%)

Abbreviation: LZD, linezolid.

Table 2. Incidence and Duration of Adverse Reactions Among Patients (N = 152)

Adverse Event	n (%)	Duration (days), Median (IQR)
Leukopenia	16(8.7)	29.0(15.3-135.0)
Hemochromatosis	42(22.8)	45.5(26.8-140.0)
Thrombocytopenia	11(6.0)	17.0(7.0-56.0)
Nausea/Vomiting	4(2.2)	44.0(17.5-82.5)
Optic Neuritis	14(7.6)	315.0(86.3-375.0)
Peripheral Neuritis	51(27.7)	120.0(90.0-165.0)
Hepatotoxicity	4(2.2)	42.0(21.0-48.0)
Nephrotoxicity	2(1.1)	70.0(56.0-84.0)
Rash	8(4.3)	35.0(11.3-104.0)

Table 3. Logistic Regression Analysis of Risk Factors for Adverse Reactions in Patients with Rifampicin-Resistant TB Treated with Linezolid

Factor	Group	Leukopenia		Hemochromatosis		Thrombocytopenia		Rash		Nausea and Vomiting		Optic Neuritis		Peripheral Neuritis		Hepatotoxicity		Nephrotoxicity	
		P value	OR (95% CI)	P value	OR (95% CI)	P value	OR (95% CI)	P value	OR (95% CI)	P value	OR (95% CI)	P value	OR (95% CI)	P value	OR (95% CI)	P value	OR (95% CI)	P value	OR (95% CI)
Sex	Male	0.002	6.279(1.916-20.582)	0.033	2.431(1.072-5.512)	0.124	2.949(0.744-11.689)	0.392	0.377(0.040-3.525)	0.649	0.562(0.047-6.737)	0.583	1.424(0.404-5.026)	0.068	0.439(0.181-1.062)	0.832	0.771(0.070-8.545)	0.996	0.000(0.000-)
	Female																		
Age		0.168	1.023(0.990-1.057)	0.080	1.020(0.998-1.043)	0.423	1.015(0.979-1.053)	0.008	1.077(1.020-1.137)	0.018	1.088(1.014-1.166)	0.417	0.981(0.938-1.027)	0.319	1.014(0.987-1.043)	0.326	0.961(0.887-1.041)	0.278	0.794(0.524-1.204)
Comorbidities	No	0.599	1.362(0.431-4.306)	0.087	2.043(0.902-4.630)	0.022	12.480(1.429-108.969)	0.803	0.807(0.149-4.361)	0.288	0.278(0.026-2.946)	0.141	2.689(0.720-10.042)	0.922	1.046(0.429-2.550)	0.996	1.3*108(0.000-)	0.994	5.6*109(0.000-)
	Yes																		
Duration		0.925	1.000(0.997-1.001)	<0.001	1.004(1.002-1.006)	0.143	1.003(0.999-1.006)	0.223	1.002(0.999-1.005)	0.521	0.998(0.992-1.004)	<0.001	1.006(1.003-1.009)	<0.001	1.005(1.003-1.008)	0.324	1.003(0.997-1.009)	0.180	1.021(0.991-1.051)

of LZD use (days)			3)								4)						8)		1)
LZD dosage (mg)	<=600																		
	>600	0.520	0.626(0.150-2.615)	0.015	3.059(1.238-7.558)	0.340	2.116(0.454-9.868)	0.243	0.230(0.020-2.706)	0.997	0.000(0.000-)	0.735	1.357(0.232-7.930)	0.997	0.000(0.000-)	0.997	0.000(0.000-)	0.998	0.000(0.000-)

LZD, linezolid; OR, odds ratio; CI, confidence interval.

Table 4. Intracellular CFU Counts Following LZD Combined with CS or CFZ in RR-TB Infection Model

	LZD + CS							LZD + CFZ						
	Pre-administration (4 h)	**Post-administration (4 h)**	**Post-administration (8 h)**	**Post-administration (24 h)**	**Post-administration (48 h)**	**F value**	**P value**	**Pre-administration (4 h)**	**Post-administration (4 h)**	**Post-administration (8 h)**	**Post-administration (24 h)**	**Post-administration (48 h)**	**F value**	**P value**
H37Rv Reference Strain														
Control Group	137±6.00	122.78±10.26	104.38±8.32	92.17±12.61	78.92±4.17	9.672	0.003	137±6.00	122.78±10.26	104.38±8.32	92.17±12.61	78.92±4.17	9.672	0.003
MIC	137±6.00	52.71±6.92	47.36±7.41	40.12±3.15	30.15±8.72	134.216	0.001	137±6.00	67.73±11.32	52.31±4.11	44.17±3.37	37.52±7.31	121.324	0.001
10MIC	137±6.00	46.32±2.78	32.97±12.03	27.69±5.31	19.32±4.09	351.647	0.001	137±6.00	56.12±4.72	47.12±1.23	34.41±7.31	28.66±4.18	278.946	0.001
20MIC	137±6.00	31.82±7.43	22.75±6.72	18.67±3.42	11.36±5.31	301.891	0.001	137±6.00	45.87±7.67	40.42±1.37	31.75±8.37	24.55±5.17	259.36	0.001
F value	-	89.267	251.348	92.246	72.314	-	-	-	78.225	189.267	87.171	53.271	-	-
P value	-	0.001	0.001	0.001	0.001	-	-	-	0.001	0.001	0.001	0.001	-	-
RR-TB Strain														
Contr	125.3	117.3	121.2	113.6	92.12	8.875	0.002	125.3	117.3	121.2	113.6	92.12	8.875	0.002

ol	3±4.6	2±6.3	7±5.3	1±3.6	±4.11			3±4.6	2±6.3	7±5.3	1±3.6	±4.11		
Group	9	1	7	7				9	1	7	7			
MIC	125.3 3±4.6 9	89.31 ±7.19	80.11 ±5.32	70.29 ±4.31	53.28 ±3.28	48.35 4	0.001	125.3 3±4.6 9	92.42 ±10.7 9	87.17 ±5.31	72.31 ±3.17	60.25 ±3.41	57.21 4	0.001
10MI C	125.3 3±4.6 9	81.62 ±5.21	68.28 ±3.69	56.31 ±3.53	47.25 ±6.24	101.3 28	0.001	125.3 3±4.6 9	85.72 ±5.73	72.69 ±3.81	66.13 ±3.35	52.25 ±6.06	107.2 36	0.001
20MI C	125.3 3±4.6 9	68.32 ±5.29	57.31 ±4.22	42.17 ±7.12	31.05 ±2.13	143.2 64	0.001	125.3 3±4.6 9	66.72 ±5.19	60.71 ±2.14	52.17 ±4.01	34.72 ±3.56	171.3 47	0.001
F value	-	34.15 2	88.43 7	52.72 3	142.5 09	-	-	-	28.34 1	98.21 2	61.46 7	137.0 15	-	-
P value	-	0.001	0.001	0.001	0.001	-	-	-	0.001	0.001	0.001	0.001	-	-

Table 5. Apoptosis Rates in RR-TB Cells Treated with LZD+CS and LZD+CFZ

Group	Time Post-infection				
	1h	3h	6h	12h	24h
RR-TB	5.01±1.07	3.72±0.47	3.19±0.32	4.52±0.74	4.18±1.06
LZD+CS	12.25±1.64	15.09±2.04	17.92±1.27	13.77±0.83	10.86±1.15
LZD+CFZ	9.71±1.63	8.67±0.98	11.36±1.08	12.35±0.81	11.60±0.87

Table 6. IL-12/23 P40 Expression in RR-TB Model Treated with LZD+CS and LZD+CFZ (pg/mL)

		Pre-administration (4 h)	Post-administration (4 h)	Post-administration (24 h)	Post-administration (48 h)	F value	P value
H37Rv Reference Strain	Control Group	693.21±87.27	662.16±32.05	746.19±13.66	701.36±5.15	6.315	0.057
	LZD+CS	693.21±87.27	742.25±36.13	784.38±13.24	789.64±10.01	0.517	0.326
	LZD+CFZ	693.21±87.27	734.61±25.31	778.06±6.17	823.53±6.08	2.361	0.027
	T value	-	-0.516	-0.621	12.356	-	-
	P value	-	0.037	0.082	0.165	-	-
RR-TB Strain	Control Group	723.36±47.25	712.33±5.31	722.91±2.86	734.07±2.60	1.320	0.631
	LZD+CS	723.36±47.25	873.36±5.62	625.16±56.02	777.26±16.15	3.031	0.041
	LZD+CFZ	723.36±47.25	886.12±10.03	779.71±30.18	741.22±20.96	0.784	0.013
	T value	-	-98.361	5.39	-1.352	-	-
	P value	-	0.001	0.001	0.093	-	-

Table 7. TNF-α Expression in RR-TB Model After Treatment (pg/mL)

		Pre-administration (4 h)	Post-administration (4 h)	Post-administration (24 h)	Post-administration (48 h)	F value	P value
H37Rv Reference Strain	Control Group	353.07±23.36	353.19±5.16	383.17±1.62	326.44±8.31	243.127	0.001
	LZD+CS	353.07±23.36	367.25±22.34	412.33±41.36	472.14±25.20	7.256	0.047
	LZD+CFZ	353.07±23.36	396.42±7.16	403.30±4.15	396.17±12.49	5.916	0.039
	T value	-	2.162	15.316	-1.415	-	-
	P value	-	0.007	0.001	0.416	-	-
RR-TB Strain	Control Group	384.01±12.33	453.08±5.31	507.39±12.76	523.17±2.16	257.048	0.001
	LZD+CS	384.01±12.33	387.15±21.46	576.19±43.16	441.46±16.07	43.169	0.006
	LZD+CFZ	384.01±12.33	432.77±6.85	601.97±24.65	581.15±24.08	17.162	0.001
	T value	-	4.167	-43.162	4.169	-	-
	P value	-	0.024	0.001	0.061	-	-

Table 8. IL-6 Expression in RR-TB Infection Model Treated with LZD+CS and LZD+CFZ (pg/mL)

		Pre-administration (4 h)	Post-administration (4 h)	Post-administration (24 h)	Post-administration (48 h)	F value	P value
H37Rv Reference Strain	Control Group	9.96±1.37	17.57±0.37	49.16±2.34	67.31±1.34	843.042	0.001
	LZD+CS	9.96±1.37	16.46±2.13	52.16±4.76	61.42±0.76	216.467	0.001
	LZD+CFZ	9.96±1.37	10.77±3.26	40.31±2.86	60.33±1.71	361.238	0.001
	T value	-	1.347	-13.469	23.467	-	-
	P value	-	0.346	0.134	0.076	-	-
RR-TB Strain	Control Group	9.34±2.72	17.19±1.03	78.36±1.71	123.50±7.16	17649.167	0.001
	LZD+CS	9.34±2.72	16.17±0.50	86.16±1.47	124.11±0.55	573.437	0.001
	LZD+CFZ	9.34±2.72	11.53±3.16	90.76±4.72	107.62±4.92	847.357	0.001
	T value	-	4.167	-123.943	6.167	-	-
	P value	-	0.042	0.004	0.076	-	-

Table 9. IL-10 Expression in RR-TB Infection Model Treated with LZD+CS and LZD+CFZ (pg/mL)

		Pre-administration (4 h)	Post-administration (4 h)	Post-administration (24 h)	Post-administration (48 h)	F value	P value
H37Rv Reference Strain	Control Group	465.34±9.55	532.17±1.07	581.82±5.13	580.05±5.16	426.164	0.001
	LZD+CS	465.34±9.55	456.01±27.16	407.51±43.16	413.49±27.19	4.167	0.076
	LZD+CFZ	465.34±9.55	527.83±5.67	574.97±37.10	571.27±3.19		
	T value	-	34.50	6.197	27.134	-	-
	P value	-	0.031	0.072	0.001	-	-
RR-TB Strain	Control Group	515.04±1.05	541.06±5.14	556.36±4.27	584.62±3.61	31.024	0.001
	LZD+CS	515.04±1.05	467.67±46.34	462.01±10.07	431.29±27.88	0.491	0.071
	LZD+CFZ	515.04±1.05	552.13±2.04	549.16±20.37	572.30±4.67		
	T value	-	3.512	12.014	18.064	-	-
	P value	-	0.072	0.005	0.001	-	-